Using LS-Dyna for Hot Stamping

Arthur B. Shapiro

LSTC

Livermore, CA, USA

Summary:

Presented is a methodology for finite element modeling of the continuous press hardening of car components using ultra high strength steel. The Numisheet 2008 benchmark problem BM03 [1] is selected as the model problem to be solved. LS-DYNA [2] has several features that are useful to numerically model hot sheet metal stamping, such as: (1) modeling high rate dynamics for press forming; (2) conduction, convection and radiation heat transfer; (3) tool-to-part contact conductance as a function of interface pressure; (4) material models that account for temperature dependent properties, phase change, phase fractions, and Vickers hardness prediction; and (5) a CFD solver for tool cooling.

Keywords:

Hot Stamping

© 2009 Copyright by DYNAmore GmbH

1 Model Problem

The continuous press hardening of a car B-pillar shown in Figure 1 was proposed by Audi as Numisheet 2008 benchmark problem BM03[1]. The process steps are:

1. Heating of the blank to 940 C.
2. Transport from the oven into the tool (6.5 s). Temperature of the blank at the beginning of the die movement, 810 C.
3. Temperature of the tools, 75 C.
4. Forming time 1.6 s
5. Quench time 20 s.

Figure 1. The problem to be solved was proposed by Audi as Numisheet 2008 benchmark problem BM03. Shown are the actual tools and the FE model.

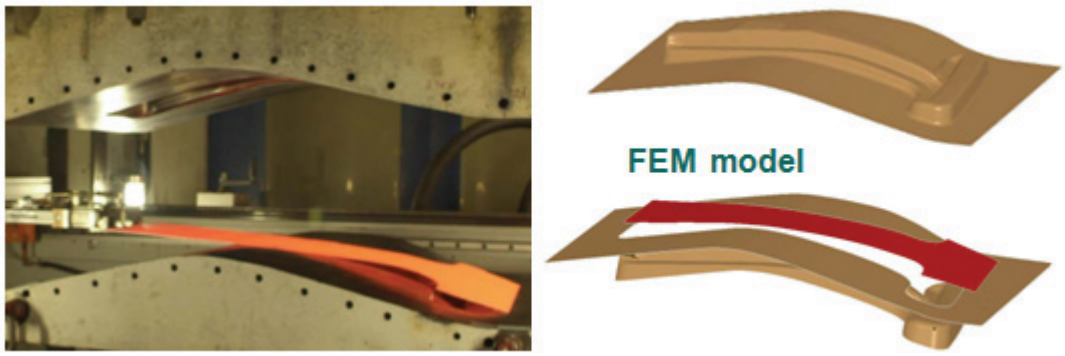

2 Material Data and Constitutive Model

There are 2 material models in LS-DYNA that are relevant to hot stamping.

1. Material model 106 (MAT-106) which is an elastic visco-plastic material model with thermal effects.
2. Material model 244 (MAT-244) which is specific to ultra high strength steels and can model the phase transformation kinetics [3,4].

Material properties used for these models are presented in the following figures and tables. Figure 2 shows stress versus strain data as a function of temperature for 22MnB5 steel at a strain rate of $0.1s^{-1}$. The Numisheet 2008 BM03 should be consulted for material property data at 2 additional strain rates. Viscous effects can be accounted for using the Cowper-Symonds [5] coefficients c and p by which the yield stress is scaled by $1+\left(\dot{\varepsilon}^{p}/c\right)^{1/p}$. C and p have strong temperature dependence (see Table 2) but are weak functions of strain rate. MAT-244 requires values for the latent heat of transformation of austenite into ferrite, pearlite, and bainite (590 MJ/m^3), and the latent heat for the transformation of austenite into martensite (640 MJ/m^3).

Table 1. Nomenclature and parameter values used in this paper.

Blank	
material	22MnB5
dimensions	
l, thickness [m]	0.00195
length [m]	1
width [m]	0.25
properties	
ρ, density [kg/m^3]	7830.
Cp, heat capacity [J/kgK]	650.
k, thermal conductivity [W/mK]	32.
α, linear expansion, [1/C]	1.3e-05
E, Young's modulus, [GPa]	100.
ν, Poisson's ratio	0.30

© 2009 Copyright by DYNAmore GmbH

Air properties at 483 C	
ρ, density, [kg/m^3]	0.471
Cp, heat capacity, [J/kg C]	1087.
k, thermal conductivity, [W/m C]	0.055
μ, viscosity, [kg/m s]	3.48e-05
β, volumetric expansion, [1/C]	1.32e-03

Figure 2. Stress versus strain data [1] as a function of temperature for 22MnB5 steel at a strain rate of $0.1s^{-1}$.

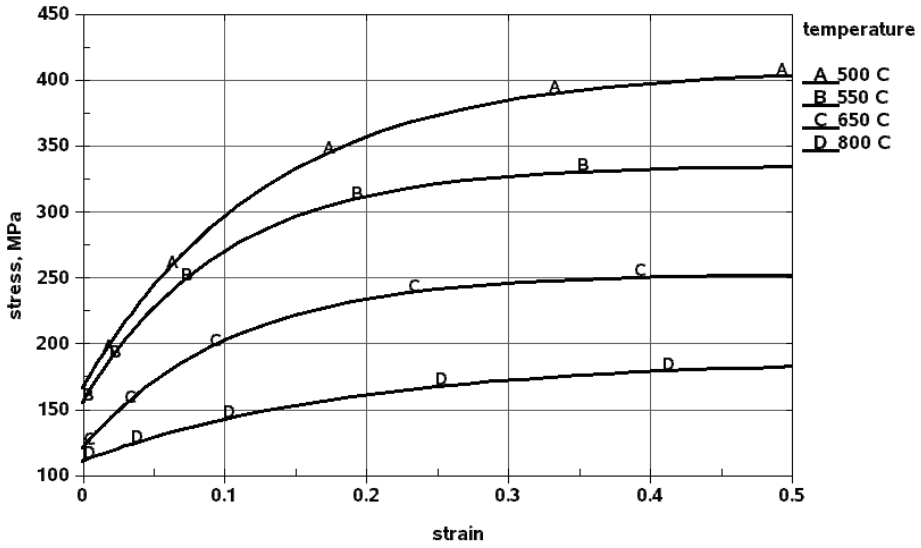

Table 2. Thermal-mechanical material properties for 22MnB5 steel [6].

Temp [C]	20	100	200	300	400	500	600	700	800	900	1000
E [MPa]	212	207	199	193	166	158	150	142	134	126	118
ν	0.284	0.286	0.289	0.293	0.298	0.303	0.310	0.317	0.325	0.334	0.343
p	4.28	4.21	4.10	3.97	3.83	3.69	3.53	3.37	3.21	3.04	2.87
c	6.2e9	8.4e5	1.5e4	1.4e3	258.	78.4	35.4	23.3	22.2	30.3	55.2
k [W/mC]	30.7	31.1	30.0	27.5	21.7		23.6		25.6		27.6
Cp [J/kg]	444.	487.	520.	544.	561.	573.	581.	586.	590.	596.	603.

3 Heating the Blank

The first step is to heat the blank from room temperature (25C) to the austenization temperature (940C). The easiest modeling technique is to define the initial temperature condition of the blank to be 940C. However, doing this will not calculate the thermal expansion of the blank between 25 C and 940 C. Therefore, the blank is heated in the FE model resulting in a thickness change from 1.95 mm to 1.97 mm.

4 Transport from the Oven to the Tool

The next step is to transfer the hot blank from the heating oven to the tools. The blank loses heat by convection and radiation heat transfer to the environment at 25C. The convection coefficient can be entered into LS-DYNA as a function of temperature defined by a data curve, or as an equation. Entering an equation allows the calculation of convection coefficients using standard empirical equations from the literature such as:

© 2009 Copyright by DYNAmore GmbH

Blank top surface $$h_{top} = \left[0.14\left(Gr * \Pr\right)^{0.33}\right]\frac{k}{L}$$ (eq. 1)

Blank bottom surface $$h_{bot} = \left[0.27\left(Gr * \Pr\right)^{0.25}\right]\frac{k}{L}$$ (eq. 2)

These equations are for turbulent free convection from a hot horizontal plate. The convection from the top surface is greater because the buoyancy driven flow is free to rise from the surface, where as it stagnates on the bottom surface. The properties for air used in calculating the Grashof number, Gr, and the Prandtl number, Pr, are evaluated at the film temperature, T_{film}. L is a length scale.

$$T_{film} = \frac{\left(T_s + T_\infty\right)}{2} = \frac{\left(940 + 25\right)}{2} = 483\ \ C$$ (eq. 3)

$$L = \frac{2\left(length * width\right)}{length + width} = 0.4\ \ m$$ (eq. 4)

$$Gr = \frac{g\beta\rho^2\left(T_\infty - T_s\right)L^3}{\mu^2} = 1.39 * 10^8$$ (eq. 5)

$$\Pr = \frac{C_p\mu}{k} = 0.687$$ (eq. 6)

The convection heat transfer coefficient is h_{top} = 8.3 W/m^2 C using equation 1. A significant concern is that these empirical formulas were developed for heat transfer at temperatures below 400C. However, a quick hand calculation reveals that radiation transport dominates at 810C to 940C and any inaccuracies in the convection coefficient will not significantly alter the results. A radiation conductance can be calculated using

$$h_{rad} = \frac{\sigma\varepsilon\left(T_1^4 - T_2^4\right)}{\left(T_1 - T_2\right)} = \frac{\left(5.67e-08\right)\left(0.8\right)\left(1213^4 - 298^4\right)}{\left(1213 - 298\right)} = 107\ \ \text{W/m}^2\ \text{C}$$ (eq. 7)

This shows that radiation heat loss is more than 10 times greater than the convection loss.

We can perform an energy balance on the blank by equating its change in internal energy to the heat loss by radiation from both sides.

$$\rho C_p V\frac{dT}{dt} = 2\sigma\varepsilon A\left(T_\infty^4 - T_{surf}^4\right)$$ (eq. 8)

This ordinary differential equation can be solved by integration between the (time, temperature) limits of (0, T_i) and (t,T_f) resulting in

$$t = \frac{\rho C_p V}{2A\sigma\varepsilon}\left[\frac{1}{4T_\infty^3}\ln\frac{\left(T_f + T_\infty\right)/\left(T_f - T_\infty\right)}{\left(T_i + T_\infty\right)/\left(T_i - T_\infty\right)} + \frac{1}{2T_\infty^3}\left(\tan^{-1}\frac{T_f}{T_\infty} - \tan^{-1}\frac{T_i}{T_\infty}\right)\right]$$ (eq. 9)

Using equation 9 and noting that V/A is the blank thickness, it takes 6.6 s for the blank to drop in temperature from T_i=940C to T_f=810C. This is in agreement with the benchmark specification that the transfer time is 6.5 s.

© 2009 Copyright by DYNAmore GmbH

A useful modeling technique is to define an "effective" heat transfer coefficient that combines both convection and radiation effects.

$$h_{eff} = h_{conv} + h_{rad} \qquad \text{(eq. 10)}$$

This is a linearization technique that will decrease computer computation time by reducing the number of nonlinear iterations that are required to achieve a converged solution. Solving the radiation transport equation is highly nonlinear due to the T^4 terms. However, making use of equation 10 we solve

$$q = h_{eff} A\left(T - T_{\infty}\right) \qquad \text{(Eq. 11)}$$

which is linear in T and is only nonlinear in h. This is easier to solve and can be modeled as a convection boundary condition with the convection heat transfer coefficient defined by (h_{eff}, T) data pairs as shown in Table 3.

Table 3: Convection, radiation and effective heat transfer coefficients

T [C]	h_{conv} [W/m^{2}C] by eq. 1	h_{rad} [W/m^{2}C] by eq. 7	h_{eff} [W/m^{2}C] by eq 11
50	5.68	5.31	11.0
100	6.80	6.8	13.6
200	7.80	10.8	18.6
300	8.23	16.3	24.5
400	8.43	23.6	32.0
500	8.51	33.0	41.5
600	8.52	44.8	53.3
700	8.50	59.3	67.8
800	8.46	76.6	85.1
900	8.39	97.2	106.
1000	8.32	121.	129.

5 Positioning and Forming

The hot blank loses heat to the environment by convection and radiation until it contacts the tools. When the hot blank (~810C) contacts the lower tool (~75C), its lower surface begins to cool due to contact as shown in Figure 3. The metal-to-metal thermal contact conductance (~2000 W/m^{2}C) is much greater than the convection (8.3 W/m^{2}C) and radiation (107 W/m^{2}C) coefficients and these modes of heat transfer become negligible. However for increased accuracy, the analysis code should have the feature to turn off thermal boundary conditions for regions in contact. There will be a through thickness temperature gradient in the blank due to the large difference in heat loss rates from the top and bottom surfaces. This is calculated in LS-DYNA using the 12 node thick thermal steel formulation developed at Lulea University [8]. This shell has 4 nodes in the plane and 3 nodes through the thickness. The 3 nodes through the thickness allows the use of quadratic shape functions to accurately calculate the through thickness temperature gradient.

Figure 3. Contact heat transfer from the blank to the tool is the dominant mode of heat transfer.

© 2009 Copyright by DYNAmore GmbH

The contact conductance is the most critical parameter controlling cooling of the blank during forming and quenching, and has the greatest uncertainty. Values are presented in [9] for several metals with various surfaces roughness as a function of interface pressure. Also, included are values when lubricants are used. Merklein [10] presents data for 22MnB5 steel at various temperatures and pressures. This data for T=550C is shown in Table 4. Shvets [11] presents the following correlations

$$h(P) = \frac{k_{air}\pi}{4\lambda}\left[1 + 85\left(\frac{P}{\sigma_r}\right)^{0.8}\right] \qquad \text{(eq. 12)}$$

Shvets' formula contains a roughness parameter, λ, and a rupture stress, σ_r. The two end points of Merklein's data can be substituted into equation 15 to calculate λ and σ_r. Then, this equation can be used to calculate h at other pressures as shown in Table 4.

Table 4. Values for contact heat transfer conductance as a function of interface pressure

P [MPa]	h [W/m^{2}C] at 550C Merklein data	h [W/m^{2}C] Shvets formula	h [W/m^{2}C] Numisheet BM03
0	750	750	1300
5	1330	1330	
10	1750	1770	
20	2500	2520	4000
35			4500
40	3830	3830	

LS-DYNA has the capability to model the mechanical coefficient of friction as a function of interface temperature and the thermal contact conductance as a function of interface pressure. Data pairs of (μ,T) and (h,T) can be entered in a table, defined by an inline function in the input file (e.g., Shvets' formula), or by a user friction subroutine for more complex models. A data table was used in this analysis with h versus pressure data pairs defined in the Numisheet BM03 benchmark specification as shown in Table 4.

There are 2 analysis techniques with increasing complexity and computer run time for the forming and quenching analyses:

1. All parts are modeled using shells. The tools are held at 75 C. The blank is modeled with a 4 node thin shell formulation that does not allow the calculation of a thru-thickness temperature gradient. Blank thickness changes are calculated. Contact conductance is a function of interface pressure.
2. The tools are modeled with solids, figure 4, allowing calculation of tool temperature changes. The blank is modeled with a 12 node thick shell formulation [8] allowing the calculation of a thru-thickness temperature gradient and thickness changes. Contact conductance is a function of interface pressure.

Table 5 contains the element count for each model and typical run times. The run times are for a double precision run on a single 2.40GHz Intel CPU DELL workstation. The number of elements used for the blank increases during the run because of mesh adaptivity to accurately calculate sharp angle changes of the mesh during deformation.

The tools in both analyses use a rigid material constitutive model. Approximating a deformable body as rigid is a preferred modeling technique in many real world applications. For example, in sheet metal forming problems the tooling can properly and accurately be treated as rigid. Elements which are rigid are bypassed in the LS-DYNA element processing algorithm and no storage is allocated for storing history variables. Consequently, the rigid material type is very CPU cost efficient. As shown in Table 5, although the tool element count increases by a factor of 7.8 between the two analyses, the CPU time only increases by a factor of 1.2.

© 2009 Copyright by DYNAmore GmbH

Figure 4. FE model using solid elements for the tools

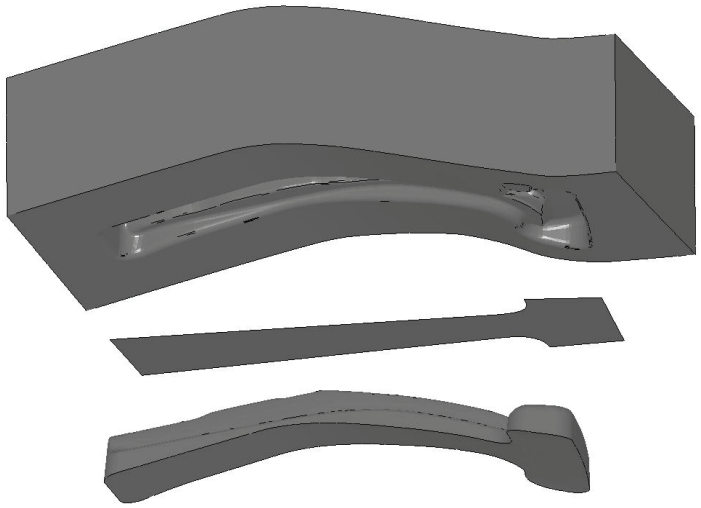

Table 5. The number of elements and computer run times.

	Analysis 1	Analysis 2
Elements used: Tool mesh Initial blank mesh Final blank mesh	 68268 shells 3096 shells 11739 shells	 532,927 solids 2096 shells 11739 shells
CPU time: Forming Quenching	 5.1 h 20 min	 5.9 h 25 min

The blank was modeled using LS-DYNA mechanical material MAT-106 which is an elastic visco-plastic thermal model. The primary reason for using this model is the ability to enter data tables of stress versus strain as a function of temperature as shown in Figure 2. These data tables were provided in the benchmark specification. Also, all other material properties (e.g., Young's modulus, coefficient of thermal expansion) can be entered as a function of temperature.

Forming results for the 2 analysis variants are presented in Table 6. There is about a 5% difference in thickness and a 2.5% difference in temperature between the 2 analyses. Figure 5 shows the thickness distribution in the blank with a range from 1.43 mm (light color) to 2.19 mm (dark color). The lightest colored regions are susceptible to tearing.

Table 6. Blank thickness and temperature results after forming

	Analysis 1	Analysis 2
Thickness minimum maximum	 1.36 mm 2.19 mm	 1.43 mm 2.19 mm
Temperature minimum maximum	 633 C 828 C	 650C 808 C

© 2009 Copyright by DYNAmore GmbH

Figure 5. Shown is the thickness distribution in the blank after forming. The range is from 1.43 mm (blue) to 2.19 mm (red).

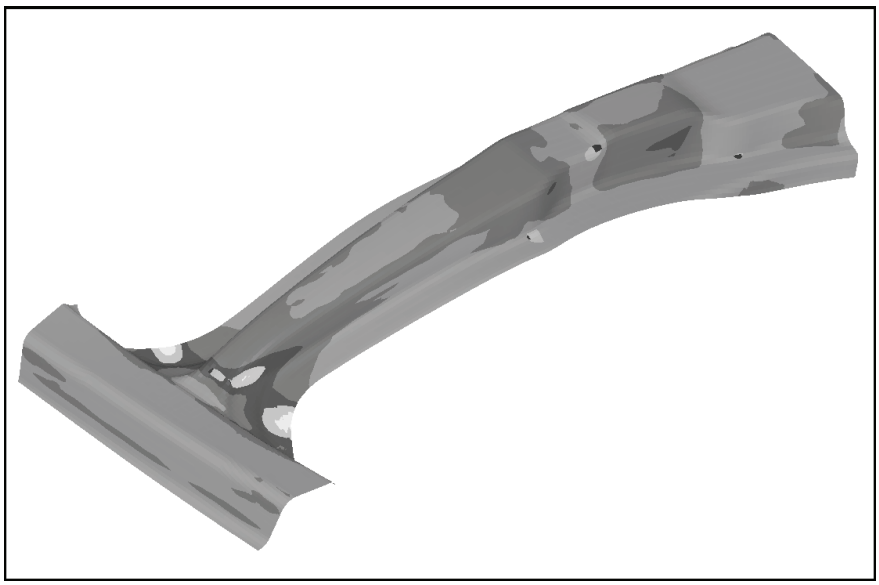

6 Quenching

The blank is held in the tools for 20 s for the quenching process. The cooling rate of the blank affects the microstructure and hardness properties of the material. Figure 6 overlays the two analysis results on a CCT diagram for a single location on the blank. Curve 1 is for the case where the tools are modeled with shells and held at 75C per the benchmark specification. Curve 2 is for the case where the tools are modeled with solids and allowed to change temperature. The results are significantly different between the two analysis variants. The reason is that in analysis 1, the tools do not change temperature and are held at 75C. This results in a faster cooling rate. The LS-DYNA thermal material model allows specification of the latent heat, 640 MJ/m^3, and the phase change temperature interval, 230-410 C for the austenite to martensite transition. Including the latent heat further slows the cooling rate. This is shown by curve 3 in Figure 6.

Figure 6. Shown is the quenching temperature history for 3 modeling scenarios overlaid on a CCT diagram for 22MnB5 steel. (1) tools modeled with shells, (2) tools modeled with solids, (3) including latent heat.

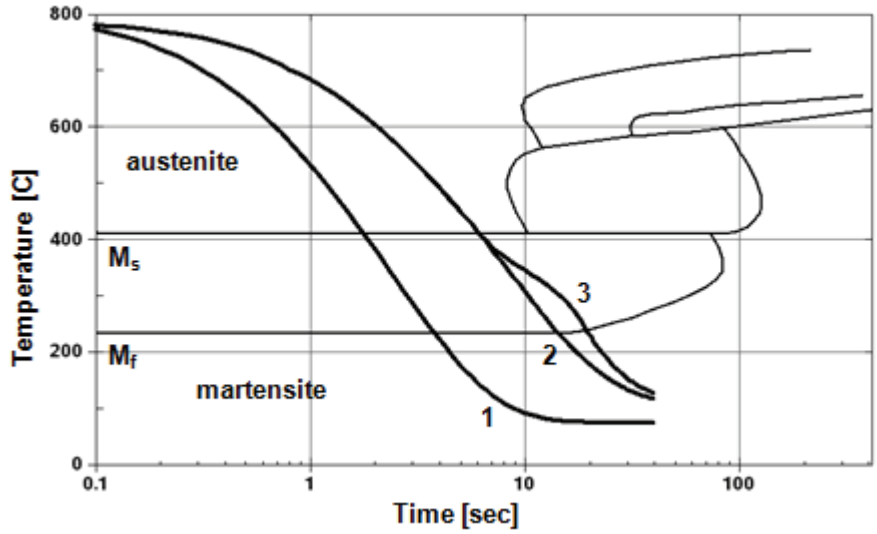

During quenching, a higher cooling rate increases the amount of martensite whereas a slower rate gives a higher content of ferrite and pearlite in the blank. LS-DYNA material mode MAT-244 [3,4] is specific to ultra high strength steels such as 22MnB5. This material model calculates the material phase fractions (Figure 7) and Vickers hardness (Figure 8) throughout the part.

© 2009 Copyright by DYNAmore GmbH

Figure 7. Martensite fraction after quenching (light grey scale=100%, dark grey scale=80%)

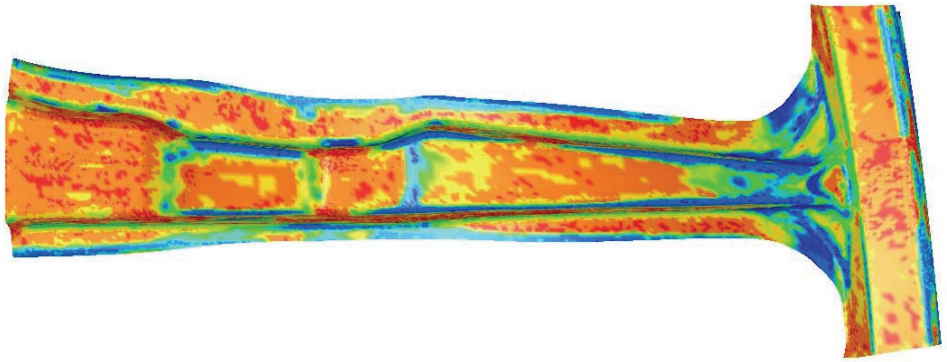

Figure 8. Vickers hardness after quenching (light grey scale=497, dark grey scale=422)

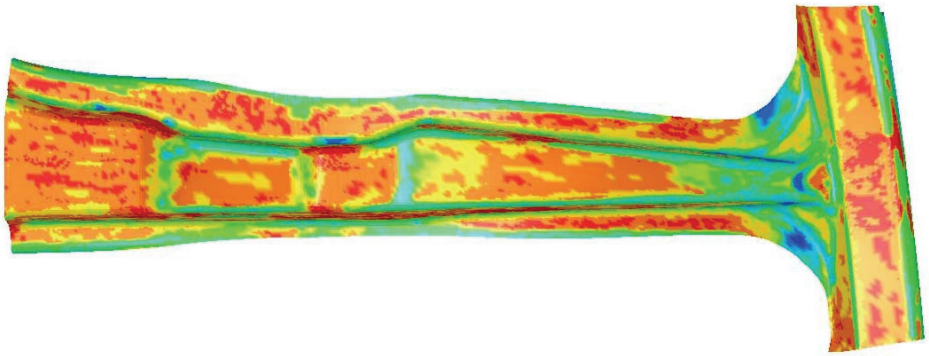

7 Literature

1. Nunmisheet 2008, The Numisheet Benchmark Study, Benchmark Problem BM03, Interlaken, Switzerland, Sept. 2008.
2. LS-DYNA Keyword User's Manual, Version 971, Livermore Software Technology Corp., Livermore, CA, USA, May 2007.
3. P. Akerstrom & M. Oldenburg, "Austenite Decomposition During press hardening of a Boron Steel – Computer Simulation and test", Journal of Material Processing Technology, 174(2006) 399-406.
4. T. Olsson, A LS-DYNA Material Model for Simulations of Hot Stamping Processes of Ultra High Strength Steels, Engineering Research Nordic AB, Sweden.
5. R.E. Cowper and P.S. Symonds, "Strain Hardening and Strain Rate Effects in the Impact Loading of Cantilever Beams", Brown University, Applied Mathematics Report, 1958.
6. D. Lorenz, private communication, DYNAmore GmbH, Stuttgart, Germany.
7. Shapiro, **"**Mysteries behind the Coefficient of Thermal Expansion (CTE) Revealed", FEA Information News, www.feainformation.com, May 2008.
8. G. Bergman and M. Oldenburg, "A Finite Element Model for Thermo-mechanical Analysis of Sheet-metal Forming", Int. J. Numer. Meth. Eng., 59, 1167-1186, 2004.
9. N. Fitzroy, Ed., Heat Transfer Data Book, General Electric Corp., Schenectady, NY, USA, 1970.
10. M. Merklein and J. Lechler, "Determination of Material and Process Characteristics for Hot Stamping Processes of Quenchenable Ultra High Strength Steels with Respect to a FE-based process Design", SAE International, SAE Technical Paper Series, 2008-01-0853, 2008.
11. I.T. Shvets, "Contact Heat Transfer Between Plane Metal Surfaces", Int. Chem. Eng., Vol. 4, No. 4, p621, 1964.

© 2009 Copyright by DYNAmore GmbH